J. Eukaryot. Microbiol., 51(4), 2004 pp. 389–393

Trichonosema algonquinensis n. sp. (Phylum Microsporidia) in *Pectinatella magnifica* (Bryozoa: Phylactolaemata) from Algonquin Park, Ontario, Canada

SHERWIN S. DESSER,[a] ANNE KOEHLER,[a] JOHN R. BARTA,[b] JUBIN KAMYAB[a] and MAURICE J. RINGUETTE[a]

[a]*Department of Zoology, University of Toronto, Toronto, Ontario, M5S 3G5, Canada, and*
[b]*Department of Pathobiology, Ontario Veterinary College, University of Guelph, Guelph, Ontario, N1G 2W1, Canada*

ABSTRACT. A new species of microsporidian, *Trichonosema algonquinensis*, is described from a freshwater bryozoan, *Pectinatella magnifica* from Ontario, Canada. The parasite develops in epithelial cells and appears as white, spherical masses throughout the tissues. *Trichonosema algonquinensis* is diplokaryotic, diploblastic and undergoes development in direct contact with the cytoplasm of the host cell. Mature spores are ovoid, tapered at one end, and measure 8.5 ± 0.3 × 4.4 ± 0.1 μm. The polar filament is wound in 20 to 23 helical coils. Although the parasite resembles *T. pectinatellae* described from the same host in Michigan and Ohio, it differs in the length of the spore and number of coils of the polar filament. Analysis of 16S rDNA by maximum likelihood, parsimony and Baysian inference, complements the morphological data in supporting the placement of *T. algonquinensis* as a sister species of *T. pectinatellae*.

Key Words. Bryozoa, Microsporia, phylogenetics, taxonomy, ultrastructure, 16S rDNA.

MICROSPORIDIAN infections in Bryozoa were first described by Korotneff in 1892, who named the spore-forming parasites he observed in *Plumatella fungosa, Myxosporidium bryozoides*. Thelohan (1895), recognizing that the parasites were microsporidians, transferred them to the genus *Glugea*. Subsequently, Labbé (1899) transferred these parasites to the genus *Nosema*. Since that time microsporidia have been described from several species of freshwater bryozoans from Europe and North and South America, but prior to 2000 only two species were named: *Nosema bryozoides* and *N. cristatellae* (Canning et al. 1997).

Canning et al. (2002), as well as Morris and Adams (2002), reviewed the literature on microsporidians of freshwater bryozoans. It has become apparent that these parasites include species of different genera. Based on morphological and 16S rDNA sequence data, Canning et al. (2002) erected two new genera and three new species of microsporidians from bryozoans in the U.S. and U.K. In the same year, Morris and Adams described a new genus and species in *Plumatella fungosa* from Scotland. Among the new genera and species described by Canning et al. (2002), was *Trichonosema pectinatellae* from *Pectinatella magnifica* collected in Ohio and Michigan.

Here we describe a new species of *Trichonosema* in *Pectinatella magnifica* from Algonquin Park, Ontario, based on light and electron microscopic features, as well as small subunit (SSU) rDNA data, which clearly differentiate it from the other described species of *Trichonosema*.

MATERIALS AND METHODS

Colonies of *Pectinatella magnifica* were collected from submerged rocks and vegetation along the shore of Lake Sasajewun, Algonquin Park, Ontario (45°35′N, 78°30′W). The bryozoans were identified by morphological features (light and electron microscopic) of their statoblasts, using the keys of Munday (1980) and Ricciardi and Reiswig (1994).

Light and electron microscopy. Portions of infected colonies exhibiting distinctive white spots were examined and photographed using an Olympus dissecting microscope equipped with a Hitachi KP-D50 digital camera. Infected tissues were squashed on a slide, examined, and photographed using an Olympus BX60 compound microscope equipped with a Hitachi KP-D50 digital camera. The length and width of 40 fresh, mature spores were measured with the aid of an ocular micrometer and the means and standard errors calculated. For transmission electron microscopy (TEM), small pieces of infected tissue were fixed at room temperature in 2.5% glutaraldehyde in 0.1 M Sorenson's phosphate buffer (pH 7.0), postfixed in 1% osmium tetroxide in the same buffer, dehydrated through an ascending ethanol series, infiltrated and embedded in Spurr's resin, and polymerized overnight at 65 °C. Semithin sections were stained with 0.2% toluidine blue, followed by 0.5% sodium borate, and photographed. Ultrathin sections stained with 3% uranyl acetate in 50% methanol and Reynold's lead citrate were examined with a Hitachi H7000 transmission electron microscope.

Amplification and cloning of SSU rDNA. Zooids from infected colonies were homogenized and processed for genomic extraction with a DNEasy Tissue Kit (Qiagen, Basel, Switzerland) according to the manufacturer's instructions. The SSU rRNA gene was amplified as a single fragment using degenerate forward (5′-GTWWKRTWCCGGAGARGGAGS-3′) and reverse (5′-ATARYGACGGGCGGTGTGTA-3′) primers. Primers were predicted manually and their identity confirmed by BLAST analysis (Altschul et al. 1990). The amplification reaction consisted of REDTaq DNA polymerase mix (Sigma, St. Louis, MO, USA), 1× amplification buffer, 1 unit Taq polymerase, 100 ng genomic DNA, 200 μM dNTPs, and 0.5 mM of each primer, in a total reaction vol. of 50 μl. Cycling parameters for amplification were as follows: denaturation at 94 °C for 15 sec, annealing at 53 °C, and extension at 72 °C for 2 min for 35 cycles. Following agarose gel electrophoresis, an approximately 1-kb amplicon was purified by means of the QiaQuick gel extraction kit (Qiagen) and cloned into the pCR2.1 cloning vector using the TOPO TA cloning kit (Invitrogen, Groningen, Netherlands). Four clones containing the 1-kb insert were sequenced in both directions by InnoBiotech (Toronto, Canada).

Phylogenetic analyses. The partial sequence of the 16S rRNA gene from *T. algonquinensis* n. sp. was aligned with 46 partial and complete sequences from microsporidia. These sequences were used to establish an initial global alignment using ClustalW (Ver. 1.83) (Thompson et al. 1994.) This primary alignment was used to find guide trees using PAUP4.0b10 (Swofford 2002) under maximum parsimony (branch and bound search with the mulpars option, equal character weighting, gaps coded as unknown, and transversions weighted 2:1 over transitions) and maximum likelihood (HKY85 model) search criteria. The guide trees were then used to select closely related taxa that should be included for examining relationships among taxa relatively closely related to *T. algonquinensis* and to determine an appropriate functional outgroup. Based on similarities between the MP and ML trees, the following taxa were assigned to the ingroup: *Antonospora scoticae* (AF024655),

Corresponding Author: S. Desser—Telephone number: 416-978-6956; FAX number: 416-978-8532; Email: wired@zoo.utoronto.ca

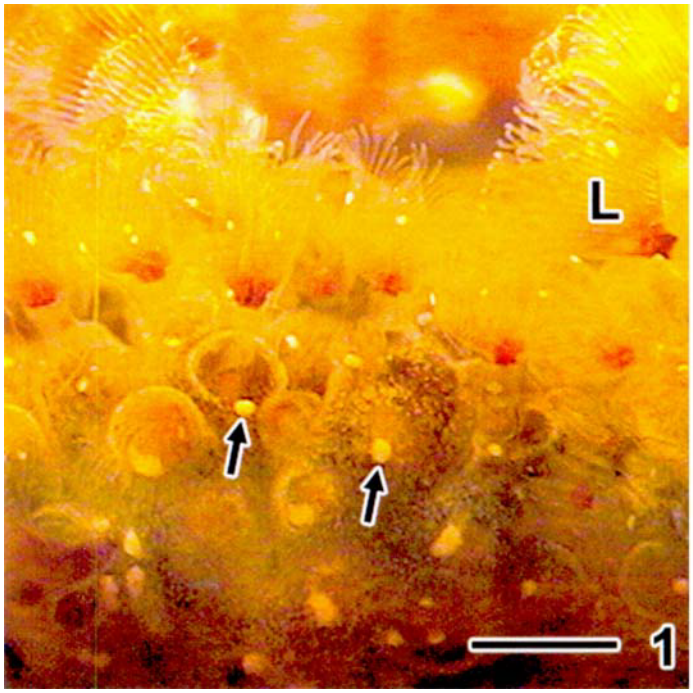

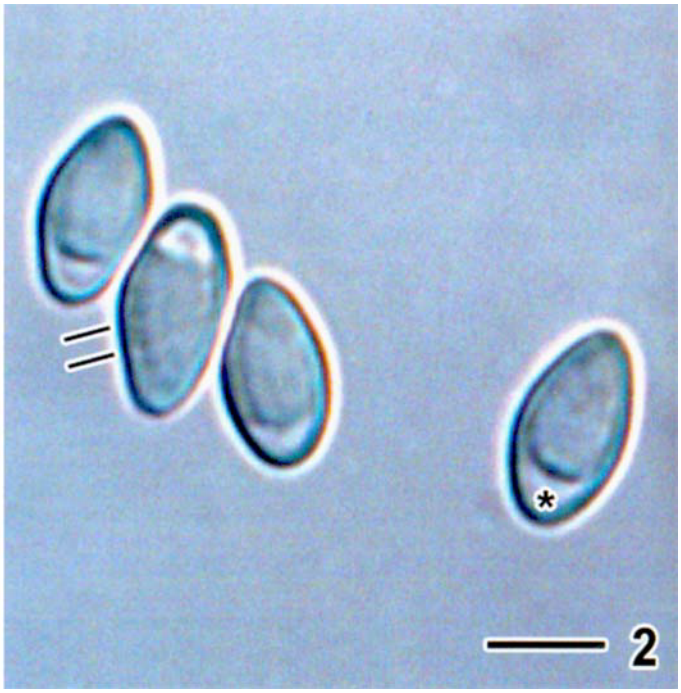

Fig. 1–2. Stages of *Trichonosema algonquinensis* from *Pectinatella magnifica*. **1.** Portion of infected colony of *P. magnifica*. Note subspherical, white patches (arrows), which demark zones of epithelium infected with *T. algonquinensis*. L = locophore. Bar = 500 μm. **2.** Fresh spores of *T. algonquinensis*. Note the coiled polar tubule (arrows), and posterior vacuole (asterisk). Bar = 5 μm.

Visvesvaria acridophagus (AF024658), *Brachiola algerae* (AF069063), *Thelohania solenopsae* (AF134205) and three clones of *Bryonosema plumatellae*; Clone 1 (AF484690), Clone 2 (AF484691), Clone 3 (AF484692); *Bryonosema tuftyi* (AF484693); *Bacillidium* sp. (AF104087); *Janacekia bebaisieuxi* (AJ252950); *Pseudonosema cristatellae* (AF484694); *Trichonosema pectinatellae* (AF484695); *Caudospora palustris* (AF132544); *Polydispyrenia simulii* (AJ29260) were selected

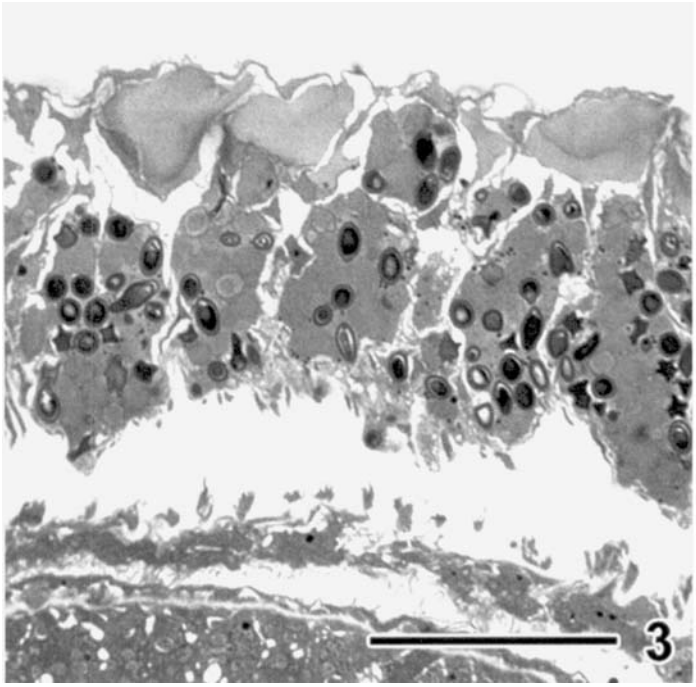

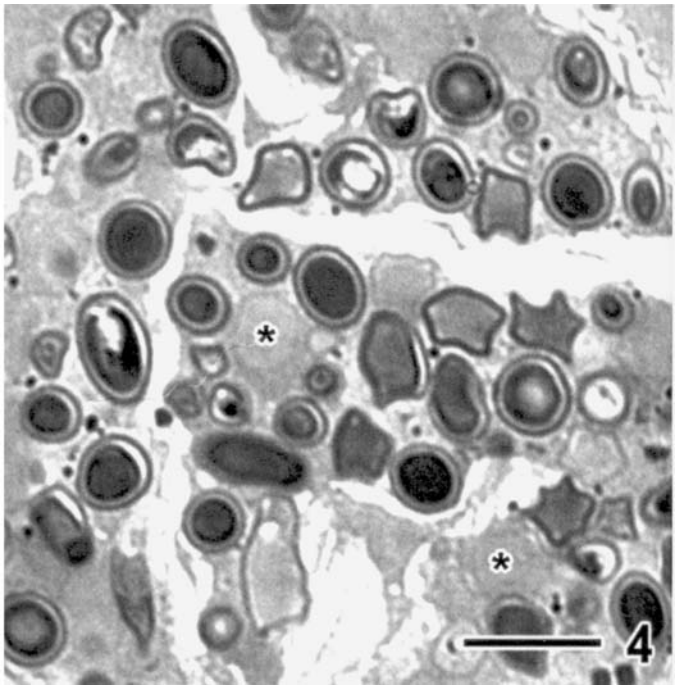

Fig. 3–4. Semithin sections of infected epithelium of *Pectinatella magnifica*. **3.** Numerous spores of *T. algonquinensis* in hypertrophied epithelial cells. Bar = 50 μm. **4.** At higher magnification, various stages of spore maturation are evident. Surrounding gray areas (asterisks) contain developing meronts and sporoblasts that are closely integrated with the cytoplasm of the host cells. Bar = 10 μm.

Fig. **5–8**. Developing stages of *T. algonquinensis* in hypertrophied epithelial cells of *P. magnifica*. **5**. Meronts (M) with diplokaryotic nuclei and developing sporoblasts (S), surrounded by punctate, dense material. Note centriolar plaque (arrow) in diplokaryotic nucleus of a meront. Bar = 5 μm. **6**. Anterior end of mature spore. Note the elaborate finger-like processes of the exospore (arrow) lying external to the continuous dense, endospore (E), which appears thinner in the apical region. A = anchoring disc. Bar = 0.5 μm. **7**. Transection through the anterior region of a mature spore illustrating the relationship between the endospore and exospore. Bar = 0.5 μm. **8**. Longitudinally sectioned mature spore. Note arrangement of the polar tubule with approximately 22 coils, some of which are in a double layer. Bar = 2 μm.

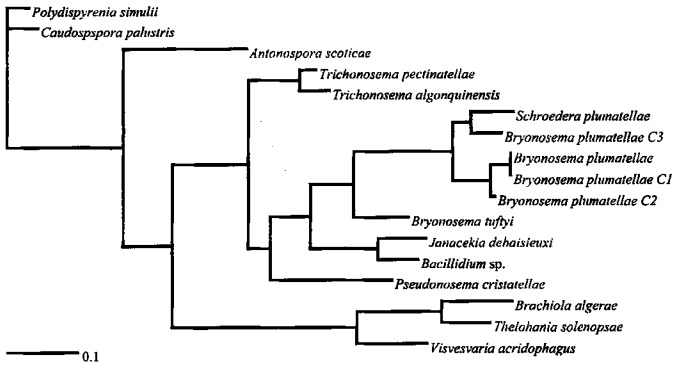

Fig. 9. Phylogram obtained by maximum likelihood analysis of 17 aligned 16S ribosomal RNA gene sequences. Branching patterns obtained by Baysian inference was identical and all nodes were supported with 100% posterior probabilities. Branch length is proportional to inferred change.

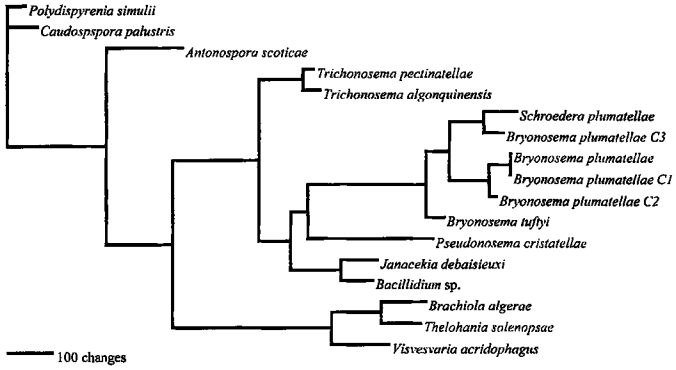

Fig. 10. Phylogram of the single most parsimonious tree obtained by maximum parsimony analysis of 17 aligned 16S ribosomal RNA gene sequences assuming a double weighting of transversions over transitions. The resulting tree had a length of 2,990 steps with a consistency index of 0.7247. Branch length is proportional to the number of hypothesized changes.

to act as outgroup taxa for analyses in which multiple outgroup taxa are permitted. For Baysian inference, *P. simulii* was used as the designated outgroup. Sequences from the 17 taxa identified as suitable for inclusion in the ingroup and outgroup were re-aligned using ClustalW using the same parameters as noted above. Phylogenetic analyses were then conducted using PAUP4.0b10 (Swofford, 2002) and MrBayes (Huelsenbeck and Ronquist, 2001).

Parsimony. Maximum parsimony analysis was accomplished using a branch and bound search algorithm with the multipars option, characters unordered and with equal weighting, gaps coded as unknown. Three branch and bound analyses were conducted with transversions weighted 1:1, 1:2 and 1:3 over transitions. For each weighting, 100 bootstrap replicates were accomplished using a branch and bound search algorithm and results expressed as a 50% majority rule consensus tree from all saved trees.

Maximum likelihood. Maximum likelihood was accomplished using an HKY85 likelihood model and the robustness of the resulting reconstruction was assessed by calculating 100 bootstrap replicates. The resulting trees were used to construct a 50% majority rule consensus tree.

Baysian inference. MrBayes was run using the general reversible model. Four Markov chains were started at random and the program was allowed to run for 1,000,000 generations with a tree sampled every 100 generations. Trees from the first 20,000 generations were discarded as a burn-in. The next 10,000 trees were saved, imported into PAUP and a 50% majority rule consensus tree was constructed.

RESULTS

Light and electron microscopy. Infected colonies of *P. magnifica* contained spherical, white masses up to approximately 0.5 mm in diam., which were scattered throughout the tissues, but located mainly around the base of the lophophores (Fig. 1). Semithin sections of infected colonies revealed that the parasites were localized in hypertrophied epithelial cells (Fig. 3, 4). Fresh spores were ovoid, tapered at one end, and measured 8.5 ± 0.3 × 4.4 ± 0.1 μm (Fig. 2). Various stages of development, including meronts, sporoblasts, and mature spores, were distinguishable by TEM. All stages of the parasite lay in direct contact with the cytoplasm of the host cell. The boundary between the meronts and host epithelial cell cytoplasm was difficult to discern (Fig. 5). Centriolar plaques were seen occasionally in the nuclear envelope of diplokaryotic meronts. A punctuated, dense layer overlying the plasma membrane delineated sporoblasts. Dense, globular processes were more numerous and closely spaced in more advanced sporoblasts (Fig. 5). Mature spores were bounded by a continuous (approximately 60 μm thick) electron-dense layer, or endospore, from which closely spaced, finger-like processes (epispore) extended (Fig. 6, 7). The endospore thinned considerably at the apex of the spore in the region overlying the ovoid anchoring disc (Fig. 6, 7). The sporoplasm was poorly preserved and the structure of the polaroplast could not be resolved. The helically wound polar tubule was arranged in 20 to 23 coils, with the anterior 5 to 6 coils in a single layer, the middle coils in a double layer, and the posterior most 5 to 6 coils, in a single layer (Fig. 8).

Phylogenetic analyses. The 17 sequences produced an alignment of 2,066 characters with 732 constant and 822 phylogenetically informative characters. Pairwise comparison between the partial (1,026 bp) sequence of *T. algonquinensis* and the 1,413 bp sequence of *T. pectinatellae* demonstrated 60 differences along the 1,026 bp aligned region (94.15% identity). The 17 aligned sequences of microsporidia were analyzed by maximum parsimony (MP), maximum likelihood (ML) and Baysian inference (BI). The branching pattern of the ML phy-

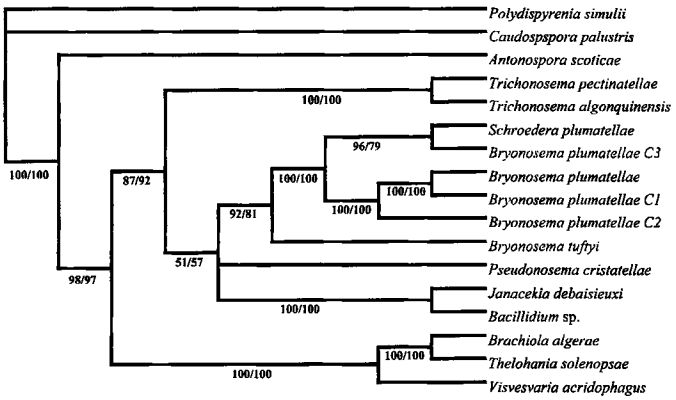

Fig. 11. Fifty percent majority rule consensus tree illustrating the bootstrap support for each clade. Bootstrap support based on maximum parsimony analysis of 17 aligned 16S ribosomal RNA gene sequences assuming a double weighting of transversion over transitions in the first number at each supported node, bootstrap support based on maximum likelihood analysis of the same sequence alignment is the second number at each supported node.

logram (Fig. 9) was identical to that of the consensus tree resulting from the BI analysis. The branching order of the BI tree was supported with 100% posterior probability at each node. Regardless of the weighting assigned to transversions (e.g. single-, double- or triple-weighted transversions over transitions), a single MP tree of identical branching pattern was obtained from each of the MP analysis, although the inferred branch lengths varied depending on the assumed transversion weighting. The phylogram resulting from double-weighted analysis (Fig. 10) differed from the ML and BI consensus trees only in the placement of *Pseudonosema cristatellae*. However, MP and ML bootstrap trees were identical in topology and only varied in the support for each clade (Fig. 11). In all bootstrap analyses (both MP and ML) as well as in the consensus trees resulting from BI, *T. algonquinensis* grouped unambiguously (100% bootstrap and 100% posterior probability support) with *T. pectinatellae*.

Diagnosis.

Trichonosema algonquinensis n. sp.
(Fig. 1–8)

Host. Pectinatella magnifica.

Locality. Lake Sasajewun, Algonquin Park, Ontario, Canada.

Prevalence. Ten of 12 colonies were infected (83%).

Site of infection. Epithelium.

Developmental stages. Diplokaryotic meronts, sporoblasts and spores in up to 0.5 mm, white patches in epithelium of bryozoan. Mature spores with dense, finger-like episporal processes; spores measure 8.5 ± 0.3 × 4.4 ± 0.1 μm. Polar tubule with 20–23 coils.

Etymology. The specific name refers to the provincial park in which the infected bryozoans were found.

Comments. Canning et al. (2002) described a new genus and species, *Trichonosema pectinatellae* infecting *Pectinatella magnifica* in Michigan and Ohio. The parasite described in this study differs considerably from *T. pectinatellae*. Spores of *T. algonquinensis* are shorter than those of *T. pectinatellae* (8.5 ± 0.3 μm vs. 9.45 ± 0.07 μm) and there are fewer coils in the polar tubule (20–23 vs. 25 or more). Moreover, *T. algonquinensis* develops in the epithelium, while *T. pectinatellae* occurs in freely circulating cells in the coelom of its bryozoan host.

Type specimens. Semithin sections and ethanol-fixed tissues of infected *P. magnifica* were submitted to the Canadian Museum of Nature, Invertebrate Zoology Collection, Ottawa, Canada, (catalogue numbers: CMNPA # 2004–001 [preserved bryozoan tissue], CMNPA # 2004–002 and CMNPA # 2004–003 [sections]). The nucleotide sequence of *T. algonquinensis* SSU rDNA has been deposited in GENBANK (Accession # AY582742).

DISCUSSION

Recent studies of Microsporidia of bryozoans by Canning et al. (1997, 2002) and Morris and Adams (2002) suggest that there are several undescribed species, and probably even genera of these parasites. Those species described thus far share several common features including large spores (longer than 7.0 μm) and upward of 25 coils of the polar tubule, that along with the localization of the parasite in the host's tissues are important in distinguishing among species. Certain ultrastructural features may be helpful, but others such as the length and configuration of the episporal processes may vary depending on the fixation protocol. Our discovery of *T. algonquinensis* supports the establishment of the family Pseudonosematidae by Canning et al. (2002) to accommodate the herewith-described microsporidian parasites of Bryozoa. The 1,026-bp sequence of the 16S ribosomal RNA gene obtained from *T. algonquinensis* showed 94.15% identity with that of the only other described *Trichonosema* species. This similarity and the consistent placement of *T. algonquinensis* as the sister taxon to *T. pectinatellae* in all phylogenetic analyses complement the morphological evidence and confirms the placement of this new species in the genus *Trichonosema*.

ACKNOWLEDGMENTS

We thank the Ontario Ministry of Natural Resources for the use of their facilities at the Wildlife Research Station in Algonquin Park. Funding for this research was provided by the Natural Science and Engineering Research Council of Canada to S. S. Desser (Grant # 6965) and M. J. Ringuette (Grant # 415144).

LITERATURE CITED

Altschul, S. F., Gish, W., Miller, W., Myers, E. W. & Lipman, D. J. 1990. Basic local alignment search tool. *J. Mol. Biol.*, **215**:403–410.

Canning, E. U., Okamura, B. & Curry, A. 1997. A new microsporidium *Nosema crsitatellae* n. sp. in the bryozoan *Cristatella mucedo* (Bryozoa: Phylactolaemata). *J. Invert. Pathol.*, **70**:177–183.

Canning, E. U., Refardt, D., Vossbrinck, C. R., Okamura, B. & Curry, A. 2002. A new diplokaryotic microsporidium (Phylum Microsporidia) from freshwater bryozoans (Bryozoa: Phylactolaemata). *Europ. J. Protistol.*, **38**:247–265.

Huelsenbeck, J. P. & Ronquist, F. 2001. MrBAYES: Baysian inference of phylogenetic trees. *Bioinformatics*, **17**:754–755.

Korotneff, A. 1892. *Myxosporidium bryozoides. Z. Wissenschaft. Zool.*, **53**:591–596.

Labbé, A. 1899. Sporozoa. *In*: Butschli, O. (ed.), Das Tierreich. Part 5. Friedlander, Berlin. p 180.

Morris, D. J. & Adams, A. 2002. Development of *Schroedera plumatellae* gen. n., sp. n. (Microsporidia) in *Plumatella fungosa* (Bryozoa: Phylactolaemata). *Acta Protistol.*, **41**:383–396.

Munday, S. P. 1980. Stereoscan studies of phylactolaemate bryozoan statoblasts including a key to the statoblasts of British and European Phylactolaemata. *J. Zool.*, **192**:511–530.

Ricciardi, A. & Reiswig, H. M. 1994. Taxonomy, distribution and ecology of the freshwater bryozoans (Ectoprocta) of eastern Canada. *Can. J. Zool.*, **72**:339–359.

Swofford, D. L. 2002. PAUP*. Phylogenetic Analysis Using Parsimony (*and Other Methods). Version 4. Sinauer Associates, Sinderland, Massachusetts.

Thelohan, P. 1895. Reserches sur les Myxosporidies. *Bull. Sci. France Belge.*, **26**:100–394.

Thompson, J. D., Higgins, D. G. & Gibson, T. J. 1994. CLUSTAL W: improving the sensitivity of progressive multiple sequence alignment through sequence weighting, position-specific gap penalties and weight matrix choice. *Nucleic Acids Res.*, **22**:4673–4680.

Received 02-01-04, 04-01-04; accepted 04-01-04